AGU PUBLICATIONS

Geophysical Research Letters

RESEARCH LETTER
10.1002/2016GL069537

Key Points:
- Tectonic tremor and low-frequency earthquakes used to extract slow slip out of the geodetic noise
- Interaseismic loading is interrupted by slow slip events that generate surface deformations less than 1 mm
- Transient stress release on many time scales shows that plate interfaces are strongly coupled where slow slip occurs

Supporting Information:
- Supporting Information S1

Correspondence to:
W. B. Frank,
wfrank@mit.edu

Citation:
Frank, W. B. (2016), Slow slip hidden in the noise: The intermittence of tectonic release, *Geophys. Res. Lett.*, *43*, doi:10.1002/2016GL069537.

Received 13 APR 2016
Accepted 12 SEP 2016
Accepted article online 15 SEP 2016

Slow slip hidden in the noise: The intermittence of tectonic release

William B. Frank[1]

[1]Department of Earth, Atmospheric and Planetary Sciences, Massachusetts Institute of Technology, Cambridge, Massachusetts, USA

Abstract Referred to as slow slip events, the transient aseismic slip that occurs along plate boundaries can be indirectly characterized through colocated seismicity, such as tectonic tremor and low-frequency earthquakes (LFEs). Using the timing of cataloged LFE and tremor activity in Guerrero, Mexico, and northern Cascadia, I decompose the interaseismic GPS displacement, defined as the surface deformation between previously detected slow slip events, into separate regimes of tectonic loading and release. In such a way, previously undetected slow slip events that produce less than a millimeter of surface deformation are extracted from the geodetic noise. These new observations demonstrate that the interaseismic period is not quiescent and that slow slip occurs much more often than previously thought. This suggests that the plate interface where slow slip and tremor occur is in fact strongly coupled and that slow aseismic release occurs over a wide spectrum of time scales.

1. Introduction

Transient aseismic slip [*Dragert et al.*, 2001] along plate boundaries represents an intermediate mode of release as the shallow brittle faulting associated with megathrust earthquakes transitions to stable sliding at greater depths [*Wech and Creager*, 2011]. Although the largest and longest slow slip events are evident on GPS displacement records [*Dragert et al.*, 2001; *Obara et al.*, 2004; *Kostoglodov et al.*, 2010], the relatively large observational noise level can hide smaller episodes of transient slip [*Frank et al.*, 2015a]. Since their discovery, these geodetically observed slow slip events are almost always accompanied by colocated recurring seismicity: tectonic tremor and low-frequency earthquakes (LFEs) [*Obara*, 2002; *Rogers and Dragert*, 2003; *Hirose and Obara*, 2005; *Shelly et al.*, 2007]. Given the more precise identification of tectonic tremor and LFEs in time and space, many studies interpret their occurrence as indirect evidence of aseismic slip [*Shelly et al.*, 2011; *Guilhem and Nadeau*, 2012; *Husker et al.*, 2012; *Wu et al.*, 2015].

We know, however, that the observed surface displacement during a slow slip event cannot fully be explained by the accumulated seismic moment of observed tremors, because the moment magnitude is often 3–4 orders smaller [*Kao et al.*, 2009; *Aguiar et al.*, 2009; *Kostoglodov et al.*, 2010]. The most likely interpretation that reconciles this discrepancy is that tremor and LFEs represent the slip that occurs on the brittle asperities along the plate interface, while slow slip events represent the deformation that happens within the aseismic matrix that surrounds these seismic asperities. A recent study validated this conceptual model for a special case in Guerrero, Mexico, by demonstrating that bursts of LFE activity with characteristic activity patterns in between previously identified slow slip are associated with small aseismic slip events hidden under the observational noise level [*Frank et al.*, 2015a]. In this study, I generalize this model and suppose that all tremor and LFE activity is coincident with slow aseismic slip. I evaluate this interpretation making use of catalogs of LFEs under Guerrero, Mexico, and tectonic tremor in the Cascadia subduction zone to analyze GPS position time series and show that there is intermittent aseismic release in between previously observed slow slip events.

2. Seismic Event Catalogs and Geodetic Data

The first study region is Guerrero, Mexico, where the plate boundary between the subducting Cocos plate and the overlying North American plate is subhorizontal at 40 km depth for more than 150 km (see Figure 1a) and provides an ideal region to study slow earthquakes. The principal slow slip cycle in Guerrero results in the largest slow slip events in the world about every 4 years [*Kostoglodov et al.*, 2010; *Radiguet et al.*, 2012] and is accompanied by both tremor and LFEs [*Payero et al.*, 2008; *Husker et al.*, 2012; *Frank et al.*, 2013, 2014].

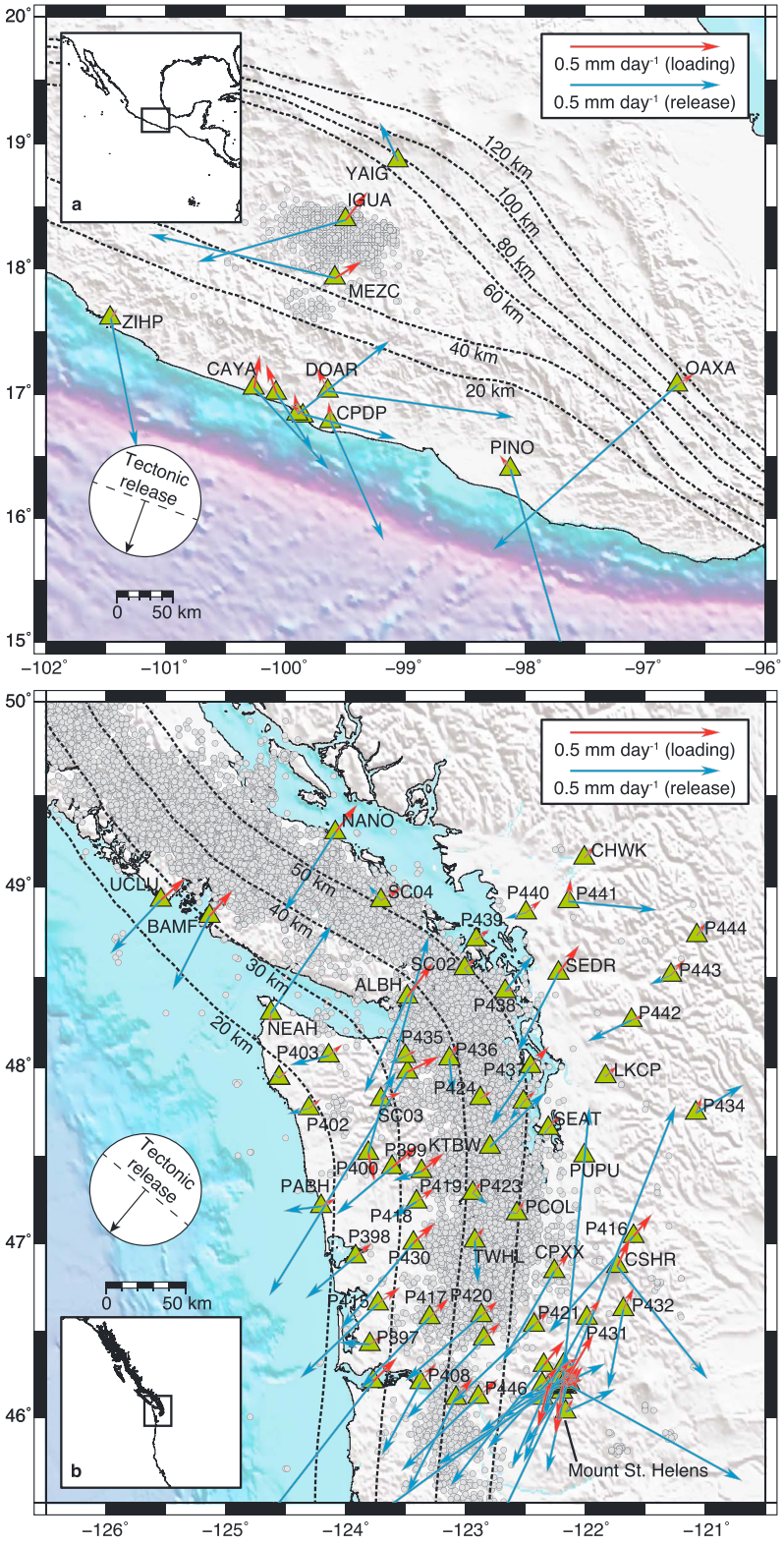

Figure 1. Decomposed tectonic loading and release velocities recorded by GPS during hidden slow slip in (a) Guerrero, Mexico, and (b) northern Cascadia. The GPS networks in both regions are shown by the green triangles. The analyzed low-frequency earthquakes (LFEs) and tectonic tremor are shown in both panels as gray points. The decomposed surface velocities during LFE (Guerrero) and tremor (Cascadia) activity are indicated by the arrows: blue for release and red for loading. The expected direction of tectonic release is shown in the white circle. The dotted contours show the slab geometry [*Audet et al.*, 2010; *Kim et al.*, 2013].

A recent effort to systematically search for LFEs in Guerrero from 2005 to mid-2007 produced a catalog of more than 1.8 million LFEs [*Frank and Shapiro*, 2014; *Frank et al.*, 2014], providing a highly detailed picture of the seismicity associated with slow slip along the subduction interface. This catalog has been used in a number of recent studies [*Frank et al.*, 2015b, 2016], including the aforementioned work that used LFEs in Guerrero as a guide to identify previously missed slow slip events [*Frank et al.*, 2015a]. The geodetic data in Guerrero are made up of continuous displacement time series on a local GPS network of 12 stations (see Figure 1a) [*Cotte et al.*, 2009].

The first reports of both deep slow slip and its correlation with tectonic tremor were discovered beneath Vancouver Island [*Dragert et al.*, 2001; *Rogers and Dragert*, 2003] in the Cascadia subduction zone, the second region studied here, where the Juan de Fuca plate plunges to the northeast underneath the North American plate. Since, there have been a number of studies dealing with both tectonic tremor and LFEs in Cascadia [e.g., *Wech and Creager*, 2011; *Houston et al.*, 2011; *Royer and Bostock*, 2014]. The tremor catalog available from the Pacific Northwest Seismic Network [*Wech*, 2010] contains almost 300,000 individual tremors spread between Northern California and British Columbia between August 2009 and December 2015. This study is limited, however, to the ~135,000 tremors that occur north of 45.5°N to focus on the slow slip that occurs underneath Vancouver Island and Washington [e.g., *Wech et al.*, 2009; *Chapman and Melbourne*, 2009]. A dense regional GPS network composed of 74 GPS stations in northern Washington and British Columbia provides good coverage of the tremor source region (see Figure 1b).

3. Extracting Slow Slip From the Geodetic Noise

3.1. Defining GPS Motion in Between Known Slow Slip Events

The GPS data analyzed here are the horizontal daily position solution time series $x_c^i(t)$ at each GPS station i and on each component c (north-south and east-west), where t is discretely sampled every day. The daily position time series are first preprocessed to remove the mean and the best fitting long-term linear trend. I then derive the GPS position to estimate the daily increment of surface motion, $\Delta x_c^i(t)$, as shown in Figure 2:

$$\Delta x_c^i(t) = x_c^i(t+1) - x_c^i(t). \tag{1}$$

The time series of displacement increments is extremely noisy, much more so than the position time series. The advantage, however, of moving from position to daily increments is that unlike position, the displacement increments can be analyzed in a noncontinuous fashion. In other words, the GPS displacement depends on previous measurements, whereas the daily increment represents the surface motion during a given day, independent of the absolute GPS position. One can therefore take any subset of discrete displacement increments at a given station and analyze them regardless of any temporal gaps in the data.

To concentrate the analysis on the motion that occurs outside of known slow slip, I first define the interaseismic as the time period between previously geodetically observed large slow slip events ($M_w > 6.0$), analogous to the interseismic period between large earthquakes. In this study, the interaseismic period that I analyze is established as the time coverage of the LFE and tectonic tremor catalogs when no detected slow slip is observed, as shown in Figure 2a and Figure S1 in the supporting information. In Guerrero I use the two previously reported slow slip cycles [*Radiguet et al.*, 2012; *Frank et al.*, 2015a]. Because the northern Cascadia subduction covers a larger geographical region over which slow slip events are known to migrate [*Wech et al.*, 2009], I allow the time periods associated with slow slip to vary over the subduction zone, identifying slow slip based on the GPS position time series at each GPS station. The interaseismic displacements increments at each GPS station and component are then computed via equation (1). Because each incremental displacement represents the motion during a given day regardless of the absolute timestamp of the measurement, I redefine the absolute time of each datum in sequential order to a relative time scale:

$$d = [0 \,..\, N], \tag{2}$$

representing each of the N days within the interaseismic period.

The surface velocity that represents the average motion per day during the interaseismic period can then be determined by the mean of the interaseismic incremental displacements:

$$\overline{v_c^i} = \frac{\sum_{d=1}^{N} \Delta x_c^i(d)}{N}. \tag{3}$$

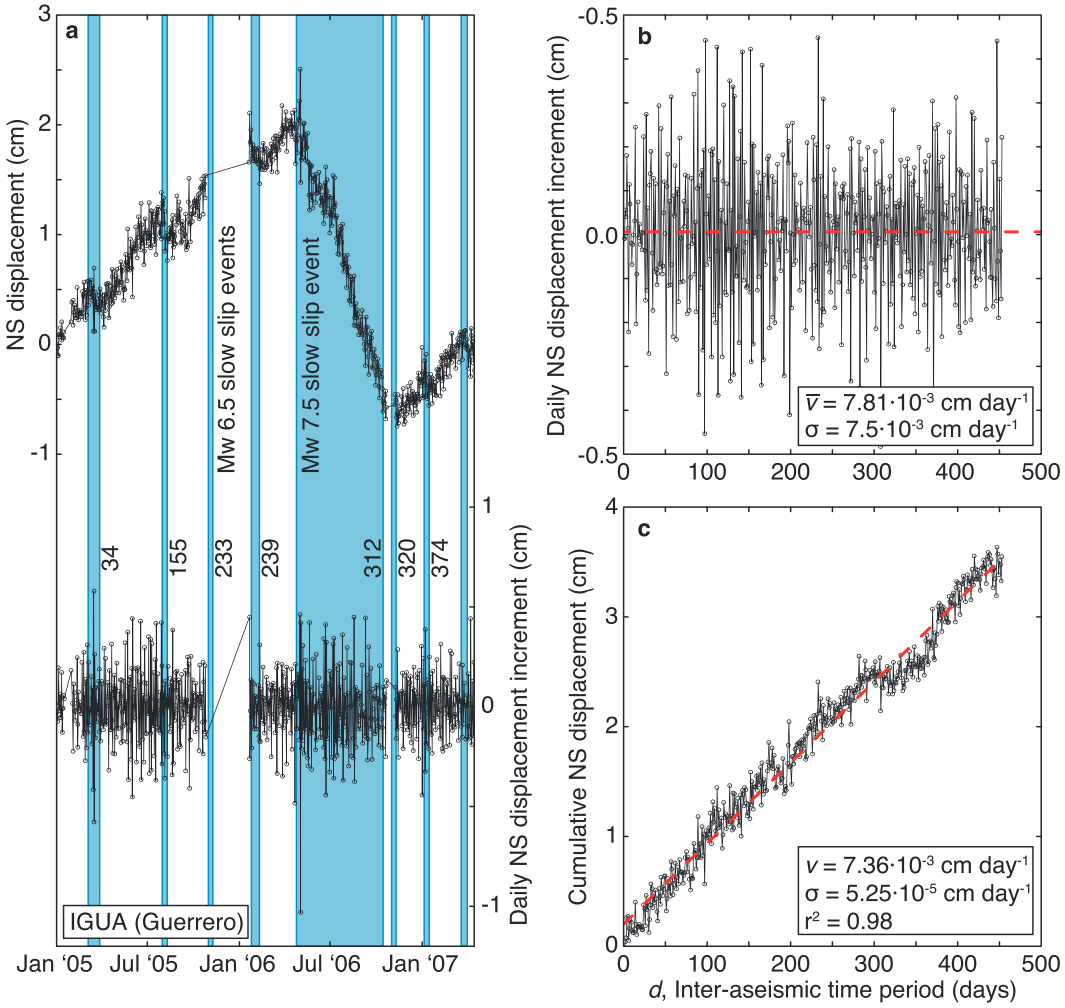

Figure 2. Extracting the average velocity during the interaseismic period at IGUA in Guerrero, Mexico. (a) First, the daily derivative of the GPS position time series (top) provides the daily displacement increment (bottom). Previously observed slow slip, shown as blue patches, is then removed from the displacement increment time series to form the interaseismic GPS daily displacement time series shown in Figure 2b. The numbers indicate the interaseismic day d (see text) after each removed slow slip event. (b) The interaseismic daily displacement increments in black are extremely noisy, and the estimated average velocity $\bar{v}$ from the mean (dashed red line) is about equal to the standard error of the mean σ. (c) The average velocity is instead estimated as the slope of the cumulative sum of the daily displacement increments, as the signal-to-noise ratio is much higher, and the standard error σ is 2 orders of magnitude smaller. This is further evidenced by the estimated linear trend (dashed red line) that explains 98% of the cumulative displacement's variance.

Figure 2b shows, however, that the signal we want to estimate, $\overline{v_c^i}$, is orders of magnitude smaller than the noise. One can, however, increase the signal-to-noise ratio by cumulatively summing the individual daily increments to compute the total displacement during the interaseismic period, as shown in Figure 2c. In such a way, the signal of interest buried in the noise will stack constructively while the incoherent noise will disappear as it sums destructively. Figure 2c shows that a linear regression of this cumulative displacement provides a more robust estimation of the average velocity than the mean of the individual daily increments (see supporting information for a more detailed discussion). As shown in Figure S1, the cumulative sum of the interaseismic displacement increments at two example GPS stations in Guerrero and Cascadia indicate a strain accumulation in the direction of tectonic convergence, as would be expected.

3.2. Decomposing GPS Time Series Into Loading and Release

I hypothesize that there are still intermittent periods of release due to undetected slow slip events within the interaseismic period and that the interaseismic period can therefore be separated into regimes of tectonic loading and release. If all periods of release associated with undetected slow slip can be removed from the

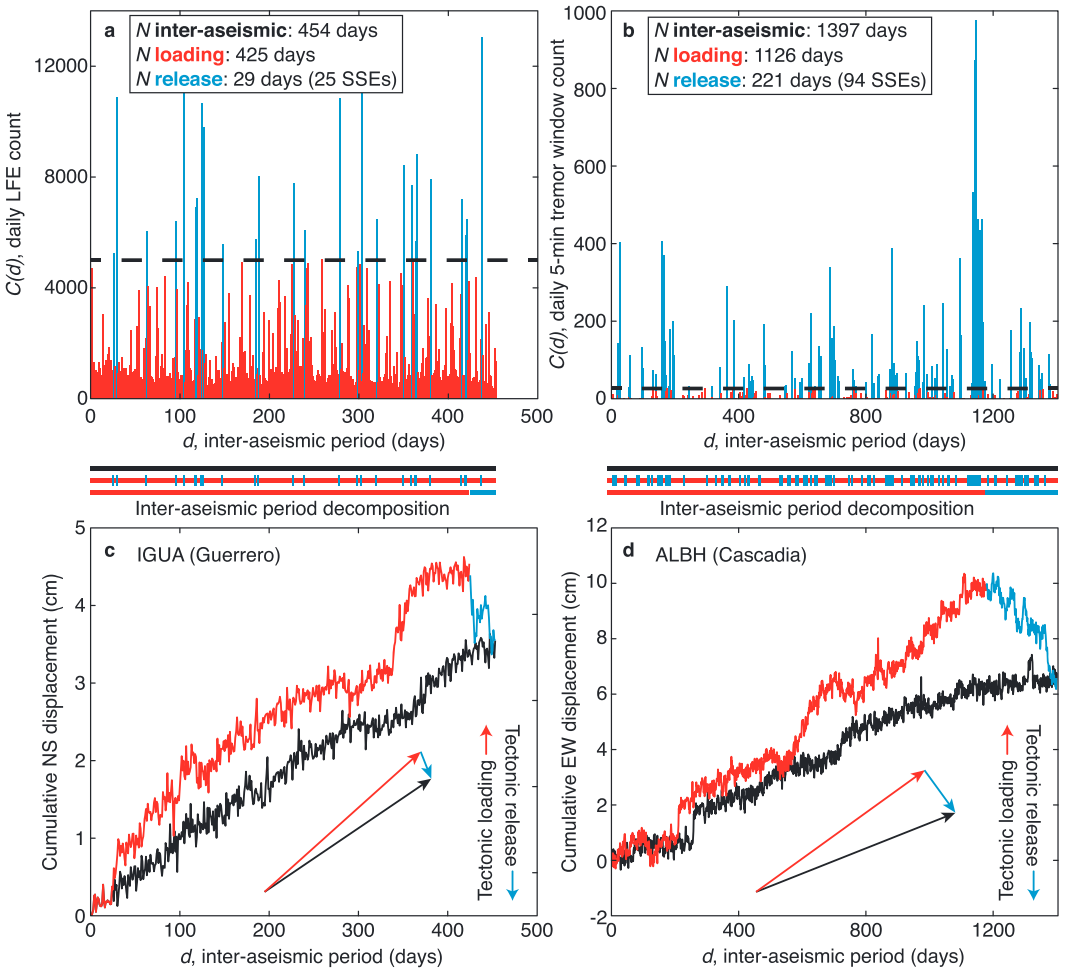

Figure 3. Decomposing the interaseismic deformation in between previously observed slow slip events. Daily seismicity counts of (a) low-frequency earthquakes in Guerrero, Mexico and (b) tectonic tremors in norther Cascadia used to decompose the interaseismic period. All days where the seismicity count is below the threshold (dashed black line) are associated with tectonic loading (red), and all days above the threshold are associated with tectonic release (blue). Consecutive days of release are considered as a single slow slip event (SSE). As shown by the diagrams between Figures 3a and 3b and 3c and 3d, days of loading (red) and release (blue) are then sorted into two separate time periods. Cumulative surface displacements recorded (c) at IGUA in Guerrero and (d) at ALBH in Cascadia before and after decomposition. The black traces show the total cumulative interaseismic surface deformation; the black trace in Figure 3c is the same trace shown in Figure 2c. The traces in red show the cumulative GPS displacement during the loading period, while the traces in blue show the cumulative GPS displacement during the release period. Note that the displacements during release (in blue) are plotted starting at the end of the decomposed loading period to highlight that the total duration of loading and release is equal to the duration of the interaseismic period. The arrow diagrams represent the linearly regressed trends after decomposition.

set of interaseismic displacement increments, then the remaining average motion should represent a faster tectonic loading than that of the full interaseismic period. Consequently, the average velocity during periods of release when slow slip is inferred to occur should be in the opposite direction of tectonic convergence.

To test this hypothesis, I decompose the interaseismic daily displacement increments into two groups based on the cataloged slow seismicity that is quantified by the daily count of tremors or LFEs, $C(d)$, for each of the N days in the interaseismic period d. I define slow seismicity here as the temporal and spatial distribution of seismic activity associated with slow slip, e.g., LFEs and tectonic tremor. This decomposition process, described in the following, is shown in Figures 3, S1, and S2. The first group that contains all of the daily displacement increments that are observed when there is more than a certain number of LFEs or tremors should represent the release of tectonic strain that I suppose occurs during the cataloged seismicity due to coincident slow slip. Although the transient slip events that potentially occur during the cataloged slow seismicity might

have different slip distributions, the average deformation during slow slip should always be in the opposite direction of tectonic motion as it represents strain release along the plate boundary. The second group contains the remaining interaseismic GPS displacement increments and should reflect the tectonic loading of the continental plate by the subducting oceanic plate. In Guerrero, a threshold of 5000 LFEs per day across the entire GPS network is used to focus on the daily displacement increments that are most likely to show tectonic release. In Cascadia, I do not define a fixed threshold across the entire subduction zone given the migration of slow slip along strike and instead adapt the threshold at each GPS station in the following manner. I first extract a subcatalog of tectonic tremor that only contains the events within 1° of latitude of the GPS station as the slow slip associated with tectonic tremor farther away will likely generate a surface displacement too small to detect. The threshold is then set as half of the median daily count of 5 min tremor time windows (as defined and identified by *Wech* [2010]). Once the displacement increments are sorted according to the above defined slow seismicity thresholds, the two groups of release and loading increments are then resampled to a relative time scale via equation (2).

While the interaseismic period and its set of daily displacement increments represent the average motion in between previously observed slow slip events, the two above defined decomposed groups GPS displacement increments, respectively, represent the average motion during and in between episodes of interaseismic slow seismicity. As discussed above, a linear regression of the accumulated displacements then yields the average surface velocity during what should be tectonic release for the first group and tectonic loading for the second. The errors in estimating the average surface velocities are shown in Figure S3 and discussed in the supporting information.

4. Results

An example at one GPS station from each study region is shown in Figures 3 and S1 where we see that the motion during slow seismicity shows a clear release of tectonic stress. Consequently, the daily displacements increments sorted into the loading group exhibit a faster convergent velocity than the average velocity observed for the full interaseismic period as predicted. I note that the time periods associated with tectonic release are often not continuous in time (as shown in Figures 3a and 3b), implying that the estimated GPS release velocity represents a surface velocity averaged over all of the slow slip events that occur during the release period.

In an attempt to estimate an average surface displacement of the interaseismic slow slip events shown in Figure 3, one could consider consecutive days of release as a single-slip transient. In this case, the GPS displacement decomposition detects 25 slow slip events over 2.5 years at IGUA in Guerrero and 94 slow slip events over 5.5 years at ALBH in northern Cascadia. Using the total cumulative release displacements in Figures 3c and 3d, the average surface displacement for the detected slow slip events would be ∼0.4 mm in Guerrero and ∼0.6 mm in Cascadia. These displacements are quite uncertain given a number of factors, such as the observational GPS error or that these detections most likely do not include the smallest transient slip events that are expected to occur if the magnitude-frequency distribution of slow slip follows a power law [*Wech et al.*, 2010]. Regardless of the uncertainties, the average surface displacement produced by the these intermittent release events are well under the geodetic noise level of ∼1–3 mm and most likely would not have been identified otherwise.

I plot in Figure 1 the average loading and release GPS velocities estimated from the linear regressions of the decomposed cumulative displacements for every analyzed GPS station in both regions. Although there is some significant scatter in the observed velocities in Guerrero, nine out of 12 GPS stations exhibit motion whose direction is more than 90° from the direction of tectonic convergence and is interpreted as release. This scatter is most likely due to the larger observational noise in Guerrero, as seen in Figure S4. The strong east-west motion that flips from east to west moving north from DOAR to MEZC is most likely explained by the recently reported sinistral strike-slip motion along the La Venta fault [*Gaidzik et al.*, 2016]. I note that the two closest stations to the LFE sources (MEZC and IGUA), where one would expect the strongest motion associated with slow slip, exhibit the largest release velocities. In northern Cascadia, there is an extremely coherent distribution of motion during tremor activity with a large majority of the 74 GPS stations showing motion toward the southwest, the direction of tectonic release. It is not surprising to see that the GPS stations close to the Mount St. Helens volcano, who are more likely to be more sensitive to volcanic processes than tectonic motion, produce erratic surface velocities. That the surface velocities at Mount St. Helens that are incoherent

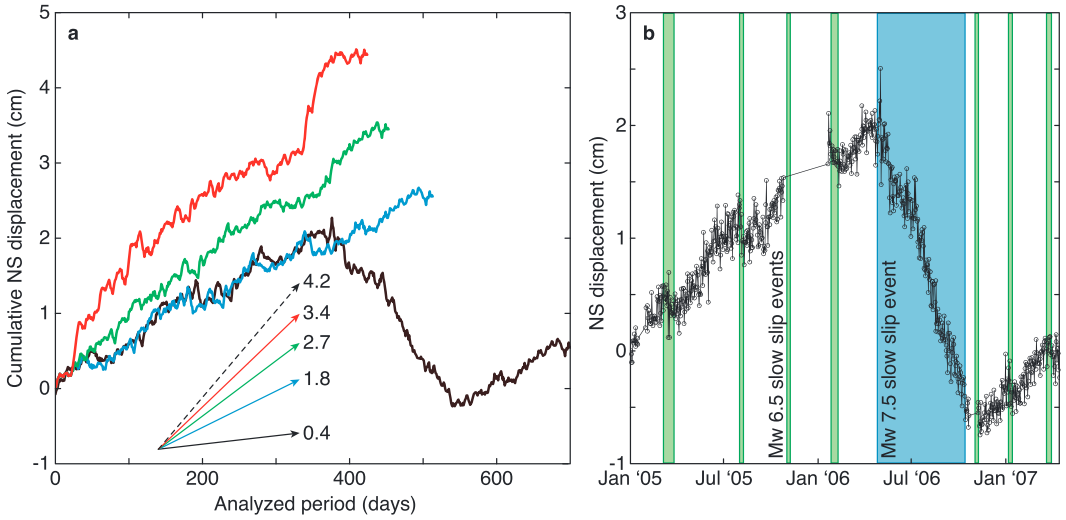

Figure 4. Stripping away the different cycles of slow slip to approach 100% plate coupling. (a) The colored lines and arrows, respectively, represent the smoothed cumulative surface displacements and average loading velocities estimated from the (b) GPS displacements recorded at IGUA in Guerrero, Mexico for different time scales of slow slip. Black trace: from 1 January 2005 to 15 April 2007 (the time coverage of the LFE catalog). Blue trace: same time period as black, but without the time window of the 2006 M_w 7.5 slow slip event [*Radiguet et al.*, 2011], shown as the blue patch in Figure 4b. Green trace: same time period as blue but without the time windows of the small 90 day slow slip events [*Frank et al.*, 2015a] indicated by the green patches in Figure 4b. Red trace: the decomposed cumulative loading displacement computed in this study (red trace in Figure 3a). The dashed arrow in Figure 4a represents the maximum theoretical loading rate at IGUA if the subduction interface was 100% coupled in both the seismogenic zone and the slow earthquake source region [*Savage*, 1983]. The numbers indicate the surface velocity in centimeters per year.

with the rest of the GPS network also demonstrate that the average surface velocities measured here do not reflect any regionally coherent geodetic noise, such as atmospheric perturbations or other common modes, that can exist in the GPS data. I note that there are a few stations, such as NEAH, that produce average release velocities in the direction of tectonic motion, but as discussed further in the supporting information, these stations mostly located close to the coast have higher levels of observational noise during the winter months most likely linked to storms. In both regions, the observed loading velocities reproduce well the direction of tectonic convergence.

5. Discussion and Conclusions

The coherent motion during LFE and tremor activity that reflects tectonic release across GPS networks in both Guerrero and northern Cascadia strongly suggests that there are many small episodes of transient aseismic slip hidden within the observational noise. This implies that one "cycle" of slow slip in a given plate segment, such as the well-known 10–14 month cycle in northern Cascadia, is not sufficient to explain the variety of time scales of transient aseismic release observed both here and in other studies [*Hirose and Obara*, 2005; *Frank et al.*, 2015a]. I therefore suggest that just as the interseismic period of the seismic cycle is never completely quiescent and is punctuated by relatively smaller seismic events, the interaseismic loading period between large slow slip events is also interrupted by smaller transient aseismic release events.

To determine the impact of the "hidden" slow slip reported here on the estimation of plate coupling, I consider in Figure 4 the evolution of the loading rate as a function of the different cycles of slow slip in Guerrero, Mexico [*Kostoglodov et al.*, 2010; *Frank et al.*, 2015a]. Given the different time scales of slow slip in Guerrero (every 4 years, every 90 days, and the hidden events identified here), I define four different times periods: (i) 1 January 2005 to 15 April 2007 (the time coverage of the analyzed LFE catalog), (ii) the same time period as (i) but removing the time window associated with the large 2006 M_w 7.5 slow slip event [*Radiguet et al.*, 2011], (iii) the same time period as (ii) but removing the time windows associated with the seven smaller 90 day slow slip events [*Frank et al.*, 2015a], and (iv) the same time period as (iii) but removing the days associated with release as defined in section 3.2 and shown in Figure 3. I then estimate the average loading rate for each of the different time periods at IGUA, the GPS station situated directly above the largest concentration of cataloged

LFE activity (Figure 1) that has been shown to be sensitive to slow slip all along the plate boundary [*Radiguet et al.*, 2011, 2012; *Frank et al.*, 2015a].

The observed loading rates in Figure 4 show that as we consider the time periods between smaller and smaller slow slip events, we arrive at a coupling of 80%, approaching the theoretical loading rate at IGUA predicted by 100% elastic coupling along the plate interface in both the seismogenic zone and the slow earthquake source region [*Savage*, 1983; *DeMets et al.*, 2010]. One can imagine that once all transient slip is identified, the estimated loading rate will be equal to the theoretical rate. If slow slip does obey a power law distribution as previously suggested [*Wech et al.*, 2010], the smallest slow slip events that escape detection could explain the 20% coupling that is still missing in Figure 4. This result shows that where slow slip, tremor, and LFEs occur, the plate boundary is in fact strongly coupled and that this coupling is broken by intermittent episodes of transient aseismic slip. I therefore suggest that the observed geodetic coupling reported along plate boundaries is biased by slow slip hidden within the noise and is systematically underestimated [*Chapman and Melbourne*, 2009; *Radiguet et al.*, 2012].

The coupling at plate boundaries has an ambiguous physical mechanism as values of coupling less than 100% can be justified either by geometrical heterogeneities along the interface that freely slip and consequently do not accumulate stress or that the loading is interrupted by undetected periods of release [*Wech et al.*, 2009; *Radiguet et al.*, 2012]. As shown in Figure 4, the results reported here support the latter interpretation and suggest that estimates of plate coupling strongly depend on the time scale used to estimate the loading rate. This conclusion therefore implies that future numerical models should not rely on a temporally fixed geometrical fault coupling with aseismic rheologies that freely slip.

Finally, I infer from these results that we currently only observe and study a small portion of the full spectrum of transient aseismic slip that occurs. As shown here, along with previous work [*Frank et al.*, 2015a], new observations of aseismic slip are possible with existing data sets when seismological information is exploited. Such interdisciplinary investigations with different data sets will most likely continue to yield results that go beyond what is possible with only one type of data.

Acknowledgments
I thank Nathalie Cotte for providing the Guerrero GPS time series. The Cascadia GPS time series was obtained through UNAVCO with support from the National Science Foundation (NSF) and National Aeronautics and Space Administration under NSF Cooperative Agreement EAR-0735156. I am grateful to everyone who participates in the maintenance of the GPS network in Guerrero, including Vladimir Kostoglodov and José Antonio Santiago. I also thank Michel Campillo, Germán Prieto, Nikolaï Shapiro, Vladimir Kostoglodov, Mathilde Radiguet, Aurélien Mordret, and Piero Poli for discussions that improved this manuscript. W.B.F. was supported by NSF grant EAR-PF 1452375. The data used are available upon request to W.B.F.

References

Aguiar, A. C., T. I. Melbourne, and C. W. Scrivner (2009), Moment release rate of Cascadia tremor constrained by GPS, *J. Geophys. Res.*, *114*, B00A05, doi:10.1029/2008JB005909.

Audet, P., M. G. Bostock, D. C. Boyarko, M. R. Brudzinski, and R. M. Allen (2010), Slab morphology in the Cascadia fore arc and its relation to episodic tremor and slip, *J. Geophys. Res.*, *115*, B00A16, doi:10.1029/2008JB006053.

Chapman, J. S., and T. I. Melbourne (2009), Future Cascadia megathrust rupture delineated by episodic tremor and slip, *Geophys. Res. Lett.*, *36*, L22301, doi:10.1029/2009GL040465.

Cotte, N., A. Walpersdorf, V. Kostoglodov, M. Vergnolle, J.-A. Santiago, and M. Campillo (2009), Anticipating the next large silent earthquake in Mexico, *Eos Trans. AGU*, *90*(21), 181–182, doi:10.1029/2009EO210002.

DeMets, C., R. G. Gordon, and D. F. Argus (2010), Geologically current plate motions, *Geophys. J. Int.*, *181*(1), 1–80.

Dragert, H., K. Wang, and T. S. James (2001), A silent slip event on the deeper Cascadia subduction interface, *Science*, *292*, 1525–1528.

Frank, W. B., N. M. Shapiro, V. Kostoglodov, A. L. Husker, M. Campillo, J. S. Payero, and G. A. Prieto (2013), Low-frequency earthquakes in the Mexican Sweet Spot, *Geophys. Res. Lett.*, *40*, 2661–2666, doi:10.1002/grl.50561.

Frank, W. B., and N. M. Shapiro (2014), Automatic detection of low-frequency earthquakes (LFEs) based on a beamformed network response, *Geophys. J. Int.*, *197*(2), 1215–1223.

Frank, W. B., N. M. Shapiro, A. L. Husker, V. Kostoglodov, A. Romanenko, and M. Campillo (2014), Using systematically characterized low-frequency earthquakes as a fault probe in Guerrero, Mexico, *J. Geophys. Res. Solid Earth*, *119*, 7686–7700, doi:10.1002/2014JB011457.

Frank, W. B., M. Radiguet, B. Rousset, N. M. Shapiro, A. L. Husker, V. Kostoglodov, N. Cotte, and M. Campillo (2015a), Uncovering the geodetic signature of silent slip through repeating earthquakes, *Geophys. Res. Lett.*, *42*, 2774–2779, doi:10.1002/2015GL063685.

Frank, W. B., N. M. Shapiro, A. L. Husker, V. Kostoglodov, H. S. Bhat, and M. Campillo (2015b), Along-fault pore-pressure evolution during a slow-slip event in Guerrero, Mexico, *Earth Planet. Sci. Lett.*, *413*, 135–143.

Frank, W. B., N. M. Shapiro, A. L. Husker, V. Kostoglodov, A. A. Gusev, and M. Campillo (2016), The evolving interaction of low-frequency earthquakes during transient slip, *Sci. Adv.*, *2*, e1501616, doi:10.1126/sciadv.1501616.

Gaidzik, K., M. T. Ramírez-Herrera, and V. Kostoglodov (2016), Active crustal faults in the forearc region, Guerrero sector of the Mexican subduction zone, *Pure Appl. Geophys.*,1–25, doi:10.1007/s00024-015-1213-8.

Guilhem, A., and R. M. Nadeau (2012), Episodic tremors and deep slow-slip events in Central California, *Earth Planet. Sci. Lett.*, *357*, 1–10.

Hirose, H., and K. Obara (2005), Repeating short-and long-term slow slip events with deep tremor activity around the Bungo channel region, southwest Japan, *Earth Planets Space*, *57*(10), 961–972.

Houston, H., B. G. Delbridge, A. G. Wech, and K. C. Creager (2011), Rapid tremor reversals in Cascadia generated by a weakened plate interface, *Nat. Geosci.*, *4*(6), 404–409.

Husker, A. L., V. Kostoglodov, V. M. Cruz-Atienza, D. Legrand, N. M. Shapiro, J. S. Payero, M. Campillo, and E. Huesca-Pérez (2012), Temporal variations of non-volcanic tremor (NVT) locations in the Mexican subduction zone: Finding the NVT sweet spot, *Geochem. Geophys. Geosyst.*, *13*, Q03011, doi:10.1029/2011GC003916.

Kao, H., S.-J. Shan, H. Dragert, and G. Rogers (2009), Northern Cascadia episodic tremor and slip: A decade of tremor observations from 1997 to 2007, *J. Geophys. Res.*, *114*, B00A12, doi:10.1029/2008JB006046.

Kim, Y., R. W. Clayton, P. D. Asimow, and J. M. Jackson (2013), Generation of talc in the mantle wedge and its role in subduction dynamics in central Mexico, *Earth Planet. Sci. Lett.*, *384*, 81–87.

Kostoglodov, V., A. L. Husker, N. M. Shapiro, J. S. Payero, M. Campillo, N. Cotte, and R. W. Clayton (2010), The 2006 slow slip event and nonvolcanic tremor in the Mexican subduction zone, *Geophys. Res. Lett.*, *37*, L24301, doi:10.1029/2010GL045424.

Obara, K. (2002), Nonvolcanic deep tremor associated with subduction in southwest Japan, *Science*, *296*, 1679–1681.

Obara, K., H. Hirose, F. Yamamizu, and K. Kasahara (2004), Episodic slow slip events accompanied by non-volcanic tremors in southwest Japan subduction zone, *Geophys. Res. Lett*, *31*, L23602, doi:10.1029/2004GL020848.

Payero, J. S., V. Kostoglodov, N. Shapiro, T. Mikumo, A. Iglesias, X. Pérez-Campos, and R. W. Clayton (2008), Nonvolcanic tremor observed in the Mexican subduction zone, *Geophys. Res. Lett.*, *35*, L07305, doi:10.1029/2007GL032877.

Radiguet, M., F. Cotton, M. Vergnolle, M. Campillo, B. Valette, V. Kostoglodov, and N. Cotte (2011), Spatial and temporal evolution of a long term slow slip event: The 2006 Guerrero Slow Slip Event, *Geophys. J. Int.*, *184*(2), 816–828.

Radiguet, M., F. Cotton, M. Vergnolle, M. Campillo, A. Walpersdorf, N. Cotte, and V. Kostoglodov (2012), Slow slip events and strain accumulation in the Guerrero gap, Mexico, *J. Geophys. Res.*, *117*, B04305, doi:10.1029/2011JB008801.

Rogers, G., and H. Dragert (2003), Episodic tremor and slip on the Cascadia subduction zone: The chatter of silent slip, *Science*, *300*(5627), 1942–1943.

Royer, A., and M. Bostock (2014), A comparative study of low frequency earthquake templates in northern Cascadia, *Earth Planet. Sci. Lett.*, *402*, 247–256.

Savage, J. (1983), A dislocation model of strain accumulation and release at a subduction zone, *J. Geophys. Res.*, *88*(B6), 4984–4996.

Shelly, D. R., G. C. Beroza, and S. Ide (2007), Non-volcanic tremor and low-frequency earthquake swarms, *Nature*, *446*, 305–307.

Shelly, D. R., Z. Peng, D. P. Hill, and C. Aiken (2011), Triggered creep as a possible mechanism for delayed dynamic triggering of tremor and earthquakes, *Nature Geosci.*, *4*(6), 384–388.

Wech, A. G. (2010), Interactive tremor monitoring, *Seismol. Res. Lett.*, *81*(4), 664–669.

Wech, A. G., and K. C. Creager (2011), A continuum of stress, strength and slip in the Cascadia subduction zone, *Nat. Geosci.*, *4*, 624–628.

Wech, A. G., K. C. Creager, and T. I. Melbourne (2009), Seismic and geodetic constraints on Cascadia slow slip, *J. Geophys. Res.*, *114*, B10316, doi:10.1029/2008JB006090.

Wech, A. G., K. C. Creager, H. Houston, and J. E. Vidale (2010), An earthquake-like magnitude-frequency distribution of slow slip in northern Cascadia, *Geophys. Res. Lett.*, *37*, L22310, doi:10.1029/2010GL044881.

Wu, C., R. Guyer, D. Shelly, D. Trugman, W. Frank, J. Gomberg, and P. Johnson (2015), Spatial-temporal variation of low-frequency earthquake bursts near Parkfield, California, *Geophys. J. Int.*, *202*(2), 914–919.